Nanosecond Time-Resolved Absorption Studies of Human Oxyhemoglobin Photolysis Intermediates

Ebrahim Ghelichkhani, Robert A. Goldbeck, James W. Lewis, and David S. Kliger
Department of Chemistry and Biochemistry, University of California, Santa Cruz, Santa Cruz, California 95064 USA

ABSTRACT The time-resolved spectra of photoproducts from ligand photodissociation of oxyhemoglobin are measured in the Soret spectral region for times from 10 ns to 320 μs after laser photolysis. Four processes are detected at a heme concentration of 80 μM: a 38-ns geminate recombination, a 137-ns tertiary relaxation, and two bimolecular processes for rebinding of molecular oxygen. The pseudo-first-order rate constants for rebinding to the α and β subunits of hemoglobin are $3.2 \times 10^4\ s^{-1}$ (31 μs lifetime) and $9.4 \times 10^4\ s^{-1}$ (11 μs lifetime), respectively. The significance of kinetic measurements made at different heme concentrations is discussed in terms of the equilibrium compositions of hemoglobin tetramer and dimer mixtures. The rebinding rate constants for α and β chains are observed to be about two times slower in the dimer than in the tetramer, a finding that appears to support the observation of quaternary enhancement in equilibrium ligand binding by hemoglobin tetramers.

INTRODUCTION

Hemoglobin consists of four subunits, two denoted α and two denoted β. The physiological role of hemoglobin is to bind molecular oxygen in the lungs and carry it to tissues throughout the body, where it is released. The efficiency with which hemoglobin accomplishes this role, in which O_2 is bound in an environment of high O_2 concentration and released in an environment of low O_2 concentration, stems from the cooperative nature of ligand binding in hemoglobin. A useful approach to understanding the association and dissociation reactions of ligands with hemoglobin has been to transiently create deoxyhemoglobin through ligand photodissociation of carboxyhemoglobin. The choice of CO as a ligand in these studies comes from the fact that the photolysis quantum yield for ligand photodissociation of HbCO is higher than that of HbO_2, and because it is more difficult to work with the oxygen derivative of hemoglobin due to its conversion into aquamethemoglobin upon exposure to ultraviolet light below 300 nm. We have overcome these problems and present in this study nanosecond time-resolved absorption spectra that report on events occurring from 10 ns to 320 μs after laser photolysis of HbO_2. Problems associated with the lower photolysis quantum yield of HbO_2 have been compensated for by increasing the laser power enough to obtain good signals but not so much as to cause damage to the protein or result in multiphoton processes. Formation of aquametHb is minimized by using a glass filter to eliminate UV light below 300 nm (Demma and Salhany, 1977, 1979; Hayashi et al., 1973).

The cooperative nature of ligand binding in hemoglobin suggests that the association and the dissociation processes for intermediates are interdependent (Pauling, 1935). Ligation states in the two-state, or allosteric, model correspond to R (relaxed) and T (tense) quaternary conformations of the protein (Monod et al., 1965). In the sequential model of Koshland et al. (1966), the association and dissociation of ligands follow a sequence of four distinct equilibrium steps corresponding to the successive binding of ligands to deoxyHb and the three partially ligated Hb species. Current models of cooperativity, common features of which provide a framework for the interpretation of events after laser photolysis of oxyhemoglobin presented here, are generally hybrids of these two models. Cooperativity in HbO_2 is manifested in the fact that the binding of a single O_2 molecule to the hemoglobin is different from the binding of O_2 to either one of the isolated α and β chains. Furthermore, because the conformational transition for oxygenated hemoglobin is slower than rebinding, nearly all of the processes that can be observed in the photolysis of oxyhemoglobin take place in the R quaternary state. This is in contrast to the HbCO system, where the conformational transition takes place along with rebinding processes after laser photolysis of HbCO (Hofrichter et al., 1983; Goldbeck et al., 1996).

In this paper we discuss the kinetics and spectra of HbO_2 photolysis intermediates. Global kinetic analysis of the observed transient spectra is carried out after least-squares smoothing and noise filtering with the singular value decomposition (SVD) method. The effect of the thermodynamic equilibrium between oxyhemoglobin dimers and tetramers on the observed spectral kinetics is investigated, and its possible significance for quaternary enhancement in hemoglobin tetramers is discussed.

Received for publication 17 January 1996 and in final form 31 May 1996.

Address reprint requests to Dr. David S. Kliger, Department of Chemistry and Biochemistry, University of California at Santa Cruz, Santa Cruz, CA 95064. Tel.: 408-459-2106; Fax: 408-459-2935; E-mail: kliger@chemistry.ucsc.edu.

0006-3495/96/09/1596/09 $2.00

EXPERIMENTAL METHODS

Materials

Hemoglobin separated from red blood cells was pelleted in liquid nitrogen, placed in small ampules, and refrigerated at −80°C (Geraci et al., 1969).

Before each experiment, 0.1 M sodium phosphate buffer at pH 7.3 was bubbled with 1 atm oxygen (Matheson Gas Products, East Rutherford, NJ) for several hours. Hemoglobin samples were prepared in the oxygen-saturated buffer solution at various desired concentrations. The concentration of heme in samples was determined using an IBM 9420 spectrophotometer (IBM Instruments, Danbury, CT). All concentrations are reported on a per-heme basis.

In most cases, samples were continuously flowed through homemade 0.5-mm to 10-mm path-length cells. Sample flow was monitored and controlled for a steady flow rate under 1 atm pressure of oxygen. We also used a commercially available 200-μm cell for high concentration measurements. Samples for this cell were prepared under 1 atm pressure of air. All experiments were run at room temperature.

Time-resolved optical density measurements

The experimental diagram for time-resolved optical density (TROD) measurements is given in Fig. 1. Oxyhemoglobin was photolyzed at a repetition rate of 1–2 Hz, using the second harmonic of a Q-switched Nd:YAG laser (Quanta-Ray/Spectra-Physics DCR-11) at 532 nm with a pulse width of 7 ns, FWHM. The detector was a microchannel plate intensified, silicon photodiode array detector (optical multichannel analyzer, OMA, model 1420 EG&G; Princeton Applied Research, Princeton, NJ) gated with an Avtech model AVL-2ps pulse amplifier (Avtech Electrosystems, Ottawa, Canada). The probe beam source was a xenon flashlamp with a 6-μs pulse width. The output of the flashlamp included light from the infrared to the far ultraviolet region of the spectrum. The ultraviolet light below 300 nm was eliminated by using a glass filter positioned between the flashlamp and the sample. The presence of strong bands in the flashlamp spectrum could limit the signal-to-noise ratio obtainable in other spectral regions, because keeping the signals from regions of high intensity within the dynamic range of the detector results in small signals in other regions. To avoid this, the flashlamp profile was leveled with two solution filters, cobalt sulfate and tris(2,2′-bipyridyl)ruthenium chloride, used after the glass filter. The flashlamp and the detector gate were both delayed relative to the laser pulse for measurements at specific times after photolysis, with the center of the gate being the reference time for delay adjustment. Synchronization of all events (laser firing, gate, and flashlamp) was established with a four-channel digital delay/pulse generator (model DG535; Stanford Research, Stanford, CA). Signals were acquired through an optical multichannel analyzer detector controller (EG&G model 1461) connected to a personal computer, which received the data for processing, averaging, and storage.

As noted in Fig. 1, a Glan-Taylor laser polarizer was used to control the polarization of the probe light at the magic angle to avoid artifacts due to rotational diffusion of the protein (Lewis and Kliger, 1991). The linearly polarized laser and probe beams were crossed in the sample cell (SC, Fig. 1). Probe light passing though the cell was then collected by a lens (L3) and focused on the slit of a spectrograph (SG). The detector was protected from scattered laser light by using a glass filter, Hoya B-390 (Hoya, Fremont, CA). Dispersed light from the spectrograph was recorded by the OMA detector.

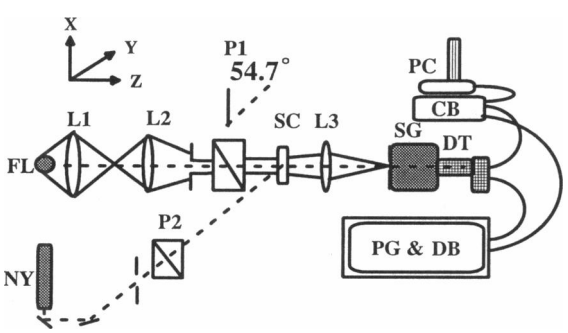

FIGURE 1 Apparatus for measurement of transient difference spectra (TROD) at magic angle. FL, probe flash lamp; NY, Nd:YAG laser; P1, Glan-Taylor polarizer rotated by 54.7° with respect to the x axis; P2, Glan-Taylor polarizer oriented along x axis; SC, sample cell; L1 and L2, collimating and focusing lenses; L3, focusing lens; SG, spectrograph; DT and CB, array detector and control box for the optical multichannel analyzer (OMA); PG and DB, pulse generator and delay systems; PC, personal computer.

Each spectrum was calculated from two computer files containing spectral data indexed by wavelength, one file containing intensities transmitted through the oxyhemoglobin solution before firing of the laser and another file corresponding to the transient species produced after laser photodissociation of the sample. For a series of n delay times the collected spectra for m wavelengths were grouped into a matrix $\{\Delta OD(\lambda_i, t_j), i = 1 \text{ to } m, j = 1 \text{ to } n\}$ for further analysis. Every spectrum in this matrix was the average of 50–64 shots. The detector gate size was kept at 20–25 ns, and a slit size of 50–100 μm was used for the spectrograph. Over the duration of an experiment, 2–4% of oxyhemoglobin was converted into metHb, and this effect was corrected for in the data matrix.

DATA ANALYSIS

Singular value decomposition

Singular value decomposition (SVD) is a mathematical method in which, given a singular matrix $\mathbf{A}$ of size $m \times n$, $\mathbf{A}$ can be decomposed into the product of three matrices $\mathbf{U}$, $\mathbf{S}$, and $\mathbf{V}^t$ of dimensions $m \times m$, $m \times n$, and $n \times n$, respectively, where $\mathbf{U}$ and $\mathbf{V}$ are orthogonal matrices and $\mathbf{S}$ is a diagonal matrix (Golub and Reinsch, 1970; Hager, 1988):

$$\mathbf{A} = \mathbf{USV}^t. \quad (1)$$

The diagonal entries of the $\mathbf{S}$ matrix are the singular values of $\mathbf{A}$, and the columns of $\mathbf{U}$ and $\mathbf{V}$ are the singular vectors of the $\mathbf{A}$ matrix. The rank of $\mathbf{A}$, s, is the number of nonzero singular values of $\mathbf{S}$ and is the size of the smallest vector space that can span the $\mathbf{A}$ matrix.

In the present application, only the first few columns of $\mathbf{U}$ contain significant spectral information. Each vector in this set corresponds to a singular value. The bigger the singular value, the more significant is the contribution of that column of $\mathbf{U}$ to the observed spectra. In practice one can use the singular value as a criterion to reject many columns of $\mathbf{U}$ as originating from experimental noise (there are other testing procedures for selecting useful singular values, such as computing autocorrelation functions for $\mathbf{U}$ and $\mathbf{V}$, but in practice the magnitudes of the singular values are typically used for assignment of a cutoff value determining the rank). The index of the smallest singular value corresponding to the significant data e is called the effective rank of the singular matrix. Subsequent calculations and lifetime fitting are done on the reduced matrices: $\mathbf{U}_r$ ($m \times e$), $\mathbf{S}_r$ ($e \times e$), and $\mathbf{V}_r$ ($n \times e$).

Time evolution of the basis spectra

Lifetime fitting is done on $\mathbf{V}_r$, the columns of which correspond to the time evolution of the corresponding columns of $\mathbf{U}_r$ (Hofrichter et al., 1983, 1985; Lambright et al., 1991). Each column of $\mathbf{V}_r$ is independently written in terms of a

linear combination of exponential functions (corresponding to first and pseudo-first-order reactions) as

$$\mathbf{V}_r(n, i) = \Sigma_j C_{ij} \exp(-t/\tau_j). \quad (2)$$

Coefficient C_{ij}, the contribution of the jth relaxation to the ith basis spectrum, is determined by a nonlinear least-squares procedure using a simplex algorithm (Dennis and Woods, 1987). [All computation and programming were done in the Matlab environment (The MathWorks, Natick, MA) using available routines.]

The noise-filtered matrix **A** is written in terms of the reduced matrices as

$$\mathbf{A} = \mathbf{U}_r\mathbf{S}_r\mathbf{V}_r^t. \quad (3)$$

Using Eq. 2 we can write $\mathbf{V}_r$ as a product of two matrices corresponding to the exponential terms and their coefficients:

$$\mathbf{V}_r = \mathbf{CE}, \quad (4)$$

where **E** is the parameterized matrix containing relaxation lifetimes and **C** is the coefficient matrix. If we insert the above expression for $\mathbf{V}_r$ into Eq. 4, we get an expression for the product of the matrices that gives the best fit to the filtered spectral matrix:

$$\mathbf{A} = \mathbf{U}_r\mathbf{S}_r\mathbf{CE}. \quad (5)$$

The residual difference between the data matrix and **A** calculated from Eq. 5 is due to experimental noise and computational tolerance.

RESULTS AND DISCUSSION

Observed lifetimes resulting from TROD

The time-resolved spectra of photolyzed oxyhemoglobin collected for delay times ranging from 10 ns to 320 μs after photolysis are shown in Fig. 2. Applying singular value decomposition analysis and relaxation lifetime fitting to the spectral matrix yielded four relaxation lifetimes, shown with their corresponding amplitudes in Table 1. These are assigned as a slow geminate recombination, a tertiary relaxation process, and two bimolecular rebinding processes of molecular oxygen to the hemoglobin molecule.

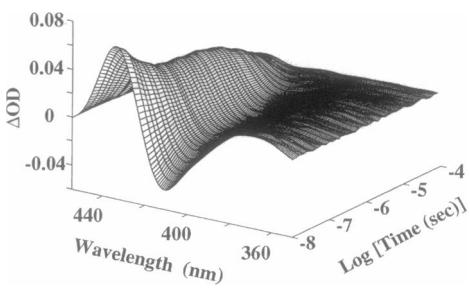

FIGURE 2 Time-resolved spectra of photolyzed oxyhemoglobin collected for delay times ranging from 10 ns to 320 μs, 10 time points per decade. Spectra were collected using the second harmonic of a Nd:YAG laser, 60-mJ pulse energy.

Geminate recombination

Geminate recombination, the recombination of photolyzed ligand before it has a chance to diffuse into solution, was first reported for hemoglobin as a nanosecond process in HbCO (Alpert et al., 1979; Duddell et al., 1979; Friedman and Lyons, 1980). From the laser photolysis of HbCO, a value of 22 ns ± 10% has been reported for the geminate recombination reaction lifetime (Hofrichter et al., 1983; Jones et al., 1992; Goldbeck et al., 1996). In contrast to the single geminate process observed in carboxyhemoglobin, oxyhemoglobin undergoes two such fast recombination processes. The first, with a lifetime of 200 ± 70 ps, is too fast to be observed in the present study (Chernoff et al., 1980; Friedman et al., 1985). A second geminate recombination phase proceeds over nanoseconds (Lindqvist et al., 1983; Friedman et al., 1985; Gibson et al., 1985). We find a value of 38 ns ± 10% for the lifetime of the slow geminate recombination of oxyhemoglobin. This relaxation shows no dependence on heme concentration (Table 1) or oxygen pressure (data not shown), as expected for a geminate process. The present study does not find large differences in the effective O_2 photolysis yields of α and β subunits, as seen in the similar amplitudes of the diffusive recombination processes for α and β chains in Table 1 at high heme concentrations (interpretation of the low-heme-concentration entries is complicated by the presence of dimers; see below). It has been found using hybrid hemoglobins that the nanosecond recombination of CO is the same for α and β subunits (Hofrichter et al., 1985; Bandyopadhay et al., 1992). However, a larger effective photolysis quantum yield for β chains has been reported after microsecond excitation of cobalt-iron oxyHb hybrids (Morris et al., 1984; Philo and Lary, 1990). At the opposite limit of very short excitation pulses, a picosecond recombination process is observed in the α chains, but not the β chains, of nickel-iron oxyHb hybrids (Shibayama et al., 1995).

It is tempting to speculate that the presence of two geminate recombinations in oxyHb, a picosecond and a nanosecond process, can be explained by hydrogen bonding between the imidazole of the distal histidine and heme-bound dioxygen. The dioxygen ligand is tilted by about 25° from the heme plane normal in the x-ray crystal structure of oxyhemoglobin and appears to form a hydrogen bond between the terminal oxygen atom and the imidazole nitrogen on the distal histidine of the α chains (Shaanan, 1982), as first proposed for oxyHb and oxyMb by Pauling (1964). The geometry of the distal histidine in the β chains, on the other hand, appears to be much less favorable for hydrogen bonding. Infrared spectroscopy of HbO_2 also shows evidence for two dioxygen conformers, with the shift in their ν(O-O) frequencies being consistent with the difference in hydrogen bonding suggested by the α and β chain x-ray structures

TABLE 1 Lifetimes (amplitudes)* for the relaxation of intermediate species formed through laser photolysis of human oxyhemoglobin at 532 nm

Process	Heme concentration			
	8 μM	80 μM	120 μM	440 μM
Slow geminate recombination	30 ns (0.54)	38 ns (0.50)	40 ns (0.28)	36 ns (0.53)
Tertiary relaxation	148 ns (0.04)	137 ns (0.05)	380 ns (0.04)	470 ns (0.03)
Rebinding to β chain	14 μs (0.06)	11 μs (0.23)	14 μs (0.34)	16 μs (0.21)
Rebinding to α chain	76 μs (0.34)	31 μs (0.25)	35 μs (0.31)	43 μs (0.21)

*Uncertainties associated with the above lifetimes (amplitudes) are approximately 10% of the tabulated numbers. For the low-amplitude processes the uncertainties might be higher than 10%.

(Alben et al., 1978; Yu, 1986). We hypothesize that dioxygens hydrogen bonded at the instant of photodissociation are more favorably oriented for fast geminate recombination than those that are not. This may arise from fast trapping of non-H-bonded dioxygens after photolysis in a heme pocket docking site that is unfavorable for rebinding to heme, such as found by Lim et al. (1995) for CO in myoglobin, whereas H-bonded dioxygens may be restrained from such trapping. Thus, the presence of two dioxygen populations, H-bonded and non-H-bonded, that do not communicate on the time scale of geminate recombination could result in the observation of two geminate rate constants. The picosecond process would correspond to recombination by hydrogen-bonded α-chain ligand, and the nanosecond process would arise from non-H-bonded ligands in either chain, consistent with the distribution of picosecond and nanosecond processes observed in the chains (Shibayama et al., 1995). A similar phenomenon is not found in the photolysis of HbCO; the absence of a picosecond lifetime and the similarity of the α and β chain geminate recombination yields observed for HbCO are explained in the above scenario by the nearly linear geometry of the Fe-C-O bond (Baldwin, 1980), which prevents hydrogen bonding with the distal histidine. It is clear in any event that geminate combination of O_2 is sensitive to a structural difference between the α and β chains that does not affect the corresponding process for CO. Access of the ligand to hydrogen bonding with distal histidine may be at least one of the structural features of Hb subunits giving rise to the pattern of chain and ligand discrimination observed in the geminate recombination process.

Quaternary and tertiary relaxation

Photodissociation of ligated oxyhemoglobin triggers a chain of events that includes tertiary relaxation. Because of the low photolysis yield employed in the present study, simple statistical considerations indicate that we are predominantly observing relaxation in and ligand recombination to the triply ligated species R_3. Thus, observation of a transition between the two quaternary structures, Hb^R and Hb^T, is statistically unlikely because R_0 and R_1 are produced only in small amounts and observation of their rapid transformation to the respective T species is masked by other processes. From the laser photolysis of HbCO it is found that the lifetime for the conformational transition between the quaternary states can be observed on time scales from 1 ms to 100 μs (Jayaraman et al., 1995; Goldbeck et al., 1996). However, no conformational transition is generally reported for HbO_2 under conditions of low photolysis at 1 atm oxygen pressure (Woodruff and Farquharson, 1978; Hopfield, 1973), and our results also show no evidence for the presence of quaternary transitions. For HbO_2 under such conditions, it is thought that the quaternary transition is widely separated in time from the time scales required for the completion of the binding reactions between O_2 and hemoglobin (Jameson and Ibers, 1994; Sawicki and Gibson, 1977; Ferrone et al., 1985). Therefore, the tertiary relaxation observed in this work corresponds to relaxation within the R quaternary conformation.

The driving force for tertiary relaxation originates from the available free energy of the photodissociated oxyhemoglobin and is stored initially as a structural change at the heme that imparts strain energy to the globin structure (Hopfield, 1973; Woodruff and Farquharson, 1978). This strain energy dissipates internally into the protein structure, affecting the observed spectra. Such relaxations are also observed for the laser photolysis of HbCO. From resonance Raman (RR) spectroscopy (Terner et al., 1981; Spiro et al., 1990), the tertiary relaxation for the HbCO molecule is first identified around 100 ns and extends into microsecond times (Goldbeck et al., 1996). From the photolysis of oxyhemoglobin we find a process with a similar lifetime, 0.1–0.5 μs, and thus assign this process to a tertiary relaxation. The low amplitude of this process (Table 1) prevented determination of the lifetime with very high precision. Moreover, the measured lifetimes in Table 1 show an apparent dependence on hemoglobin concentration, unexpected for an intraprotein relaxation, that is probably an artifact of the solution conditions, as further discussed below.

Bimolecular binding of oxygen

In addition to the geminate recombination and tertiary relaxation processes, Table 1 indicates that we also observed two microsecond lifetimes for the binding of O_2 to the hemoglobin. The faster process was assigned by Gibson (1973) as rebinding to the β chain of hemoglobin and the second as rebinding to the α chain of hemoglobin, based on

analogy to the assignment for the slowly binding *n*-butyl isocyanide ligand. The assignment of distinct rebinding rates for α and β chains within the tetramer is also consistent with the small difference in O_2 binding rate constants observed for the isolated chains (Noble et al., 1969) and is confirmed for the tetramer by studies of hemoglobin valence hybrids (Philo and Lary, 1990). Lifetime values of about 8–10 μs and 28–35 μs are generally reported for the β and α recombination processes, respectively (Noble et al., 1969; Jameson and Ibers, 1994). Here, these two lifetimes are found to be 11 μs (apparent rate constant of 9.4×10^4 s^{-1}) and 31.0 μs (apparent rate constant of 3.2×10^4 s^{-1}), respectively. The amplitudes of these two processes are smaller than that of the nanosecond geminate recombination reaction. Table 1 shows that these rate constants are independent of hemoglobin concentration above a heme concentration of 80 μM, whereas at 8 μM the rebinding to the α chain appears to be significantly slower (see below).

Absorption profiles of the intermediate species

From the results of the SVD analysis of the spectral matrix we have found three basis spectra. These spectra, the first three vectors of the **U** matrix, when multiplied by the corresponding singular values and the time courses of the spectra, give a best representation, in a least-squares sense, of the observed spectral matrix. This indicates there are at least three major absorption profiles in the Soret region, shown in Fig. 3 *a*. These are the first three **U** vectors multiplied by the square roots of their corresponding singular values divided by the largest singular value. The highest amplitude component looks like a deoxy-oxy difference spectrum. In Fig. 3 *b*, the first three components of the **V** matrix are plotted as a function of logarithm of time. These curves are the time courses of the first three components of the **U** matrix. The most significant spectral information is carried by the **V1**, and this vector makes the greatest contribution to the global fitting of the lifetimes.

Conversion of the difference spectra from Fig. 2 into absolute spectra is useful for structural analysis using time-resolved spectra collected under conditions that are fixed except for the delay times. To obtain the time-resolved absolute absorption spectra, the steady-state equilibrium oxyhemoglobin spectrum, $A_{in}(\lambda, 0)$, is used to convert the difference spectra into the absorption profiles by

$$\mathbf{A}_f(\lambda, t) = (\phi)^{-1}\Delta\,\mathrm{OD}(\lambda, t) + A_{in}(\lambda, 0), \qquad (6)$$

where $A_f(\lambda, t)$ is the absolute transient absorption profile for delay time t, and $\Delta\mathrm{OD}(\lambda, t)$ is the measured difference spectrum. Transient absorption is defined by $A_f(\lambda, t) = -\log_{10}(I/I_i)$ and $A_{in} = -\log_{10}(I_i/I_o)$, where I, I_i, and I_o are the transmittances corresponding to the transient intermediate, equilibrium oxyhemoglobin, and cell without sample, respectively. Parameter ϕ is the photolysis yield. We have found an approximate value of 15.3% for ϕ by comparing the ratio of the absorptions, at λ_{max}, for the first and the last

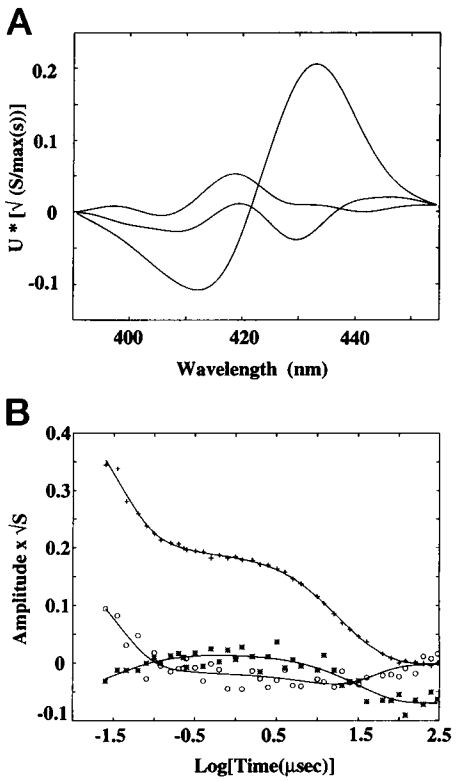

FIGURE 3 (*a*) First three columns of the U matrix. These three spectra correspond to the three largest singular values (diagonal elements of **S** matrix). Each column is multiplied by the square root of its singular value normalized to the largest singular value (first element of **S**). The amplitudes of these plots are related to their contributions to the observed time-resolved spectra. (*b*) First three columns of **V** matrix are plotted as a function of $\log_{10}$ (s). Experimental points are indicated by the cross, star, and circles. Amplitudes in this figure are multiplied by the square roots of the corresponding singular values. The curves passing through the experimental points are the results of global fitting.

spectra with those of the normal deoxy- and oxyhemoglobin at the same heme concentration. This is an approximate value that is consistent with the photolysis yield for HbO_2 reported by Duddell et al. (1980).

Six absorption spectra, generated using the above method, are shown in Fig. 4. The first spectrum belongs to the intermediate species produced after photolysis, which apparently arises from both geminately dissociated oxyhemoglobin and activated hemoglobin resulting from the photolysis of HbO_2, [Hb···O_2] and Hb(R_3)*. Internally activated hemoglobin produced by the complete photolysis of liganded hemoglobin, Hb*, was initially reported by Gibson (1959) to have an absorption profile different from that of normal deoxyHb, and has since been identified as unliganded protein that has not relaxed from the R-state conformation of liganded Hb (Scott and Friedman, 1984). Gibson's activated deoxyhemoglobin was the result of photolysis probing on a microsecond time scale and thus would correspond in the context of the present study to the conformational species produced by tertiary relaxation from the nanosecond Hb* species shown in Fig. 4. The absence of an

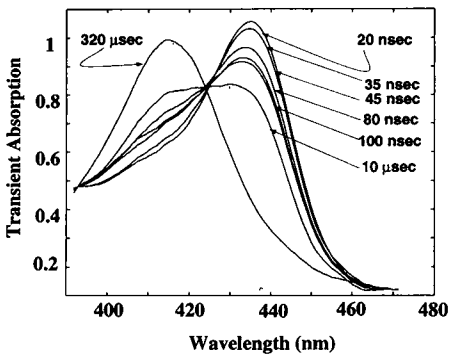

FIGURE 4 Absolute transient absorption spectra of photoexcited oxyhemoglobin at different delay times. The delay time for each spectrum is indicated in the figure.

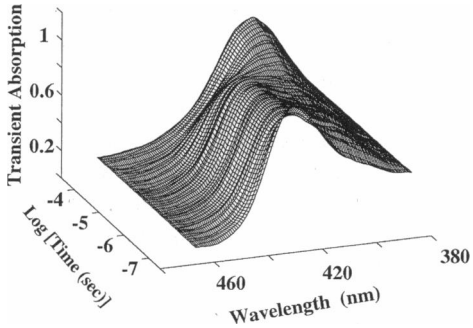

FIGURE 5 Three-dimensional plot of time-resolved transient absolute absorption spectra of the photolyzed oxyhemoglobin collected for delay times ranging from 20 ns to 320 μs, 10 time points per decade.

isosbestic point in Fig. 4 reflects spectral changes in the deoxy band (primarily a small blue shift) accompanying geminate ligand escape from [Hb···O_2] to form Hb(R_3)* and the subsequent tertiary relaxation of the latter.

The transient absorption spectrum with the broadest profile in Fig. 4 belongs to the mixture of species present at the 10-μs delay time. This spectrum corresponds to the point at which half of the hemes are religated with oxygen, as this spectrum can be approximately duplicated by mixing equal amounts of the oxy and deoxy absorption spectra. The spectrum does not evolve beyond that present at 320 μs, so the 320-μs spectrum belongs to that of fully oxygenated hemoglobin. In fact, the position and spectral profile of this spectrum are identical to those of equilibrium oxyhemoglobin, indicating that there is no permanent change in the structure of the final product.

The spectrum of the immediate photoproduct has its maximum absorption at λ_{max} = 437 nm, whereas for the spectrum of fully oxygenated hemoglobin the maximum absorption is 415 nm. The energy separation between these two maxima (1261 cm^{-1}) is larger than the difference between equilibrium deoxyhemoglobin and oxyhemoglobin by about 360 cm^{-1}. This difference is clearly due to the accessibility of different internal states for the immediate photoproduct in comparison with static deoxy hemoglobin. However, in going from the first spectrum to the last spectrum there are species that have a combination of spectroscopic features that lie between the deoxy-looking first spectrum and the last spectrum of fully oxygenated hemoglobin. As mentioned above, the intermediate spectra do not correspond exactly to linear combinations of the first and last spectra, reflecting the partial relaxation of conformational state differences between the photoproducts and equilibrium deoxyHb.

The overall time-resolved surface of the transient absorption profiles collected for the oxyhemoglobin sample of heme concentration equal to 80 mM is shown in Fig. 5. The salient feature of this surface is that it displays the transition from the initial photoproduct to the final recombined HbO_2 in terms of absolute absorption profiles containing both kinetic and spectral information for the intermediates resulting from photolysis of the oxyhemoglobin. The ligand recombination and protein relaxation processes evident in Fig. 5 have been discussed to this point exclusively in terms of the Hb tetramer, but the effect on these kinetic processes of subunit dissociation to produce liganded dimers may also be significant, particularly at lower heme concentrations, and this issue will now be examined.

Concentration dependence of the photoproducts

A solution mixture of hemoglobin and molecular oxygen is composed of several species at equilibrium, the concentration of these species being dependent on the oxygen and heme concentrations. The question is, what is the possible contribution of these equilibrium species to the observed spectra resulting from the laser photodissociation of HbO_2? The detailed thermodynamic properties of oxygen/hemoglobin mixtures have been studied extensively (Alberty, manuscript submitted for publication; Mills et al., 1976; Johnson et al., 1976). There are eight reactants in the equilibrium state of the oxygen/hemoglobin system that correspond to seven equilibrium reactions. The equilibrium constants for these reactions depend on the temperature, pressure, pH, and ionic strength (Alberty, manuscript submitted for publication; Sawicki and Gibson, 1981). For our experiment and in the following discussion, all variables are fixed, except for the concentrations of oxygen and heme. A computational method for the general problem of calculating equilibrium composition of a complex reaction was developed by Krambeck (1991). We used a code based on this approach introduced by Alberty in a recent study of the thermodynamics of molecular oxygen binding to hemoglobin (Alberty, manuscript submitted for publication; Alberty, 1991).

For the equilibrium mixture of the oxygen/hemoglobin system corresponding to an O_2 concentration of 1.5×10^{-3} M and a heme concentration of 80 μM, the equilibrium concentration of the fully ligated hemoglobin tetramer, $(\alpha\beta)_2(O_2)_4$, is 71.2 μM and the ligated hemoglobin dimer, $\alpha\beta(O_2)_2$, is 8.8 μM, with the fractional saturation of the

sample equal to 0.999. To explore the effect of heme concentration on the equilibrium compositions of dimeric and tetrameric hemoglobin we made a series of calculations for heme concentrations ranging from 8 to about 700 μM, keeping the oxygen concentration fixed at 1.5×10^{-3} M, the results of which are shown in Fig. 6. We see from these two curves that the concentration curve of fully ligated dimer has a very small slope in comparison with that of the fully ligated tetramer. Despite the fact that the ratio of dimer to tetramer decreases as a function of heme concentration, this ratio does not vanish, even for very high values of heme concentration. Therefore, under no experimental condition is it possible to reach a 100% concentration of fully oxygenated dimer or tetramer alone. This is because of the nature of the reactants and the energetics of the equilibrium reactions, ΔG_{Rx}. However, one can maximize or minimize the dimer/tetramer ratio, as shown in Fig. 6.

To elaborate the possible role of dimer contributions on the two ligand-binding rates, we varied the heme concentration as suggested by Fig. 6. First, two HbO_2 samples of higher heme concentration were prepared: 120 μM and 440 μM. The two pseudo-first-order lifetimes of the rebinding to α and β chains were found to vary little with concentration (see Table 1). At these concentrations, the percentage of dimer is small and its spectral effect, if any, is negligible. The percentages of dimer to tetramer computed using the procedure of Alberty are 8.5% and 4.8%, respectively (Alberty, manuscript submitted for publication; Krambeck, 1991). Although the above two rates appear to decrease slightly with increasing heme concentration, the change in rate constants does not suggest any significant contribution from the low percentage of dimer present in the samples, for two reasons. First, given the size of the uncertainty in lifetimes (~10% for the large amplitude processes), the differences may not be statistically significant. Second, the higher heme concentration is close to the concentration of O_2, a situation that is expected to give a deviation from pseudo-first-order kinetics that can artifactually lengthen the observed lifetimes obtained from exponential fitting.

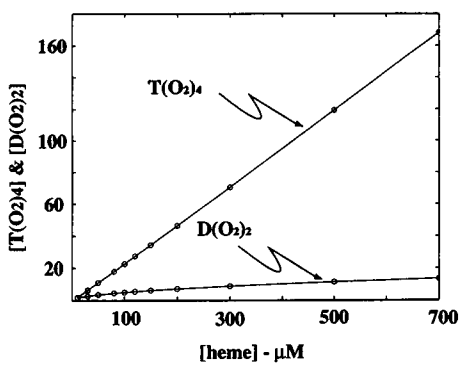

FIGURE 6 Calculated equilibrium compositions of fully oxygenated dimer and tetramer mixtures plotted as a function of heme concentration. Concentration of O_2 is fixed at 1.5 mM as heme concentration is varied from 8 to 700 μM.

Relatively larger changes were observed for the lifetime of the tertiary relaxation process at higher heme concentrations in Table 1, but these are small-amplitude processes with higher relative uncertainties compared with those of the larger amplitude processes. Large uncertainties are also encountered in lifetime fitting within this time regime for HbCO (Hofrichter et al., 1983), wherein both a 100-ns and a 1-ms process have been resolved (Goldbeck et al., 1996). Given the large uncertainty in fitting the lifetime of a small-amplitude process in a time regime that may, by analogy with HbCO, actually contain at least two distinct relaxations, and given the further likelihood of "cross-talk" in the lifetime fitting between this process and the large-amplitude recombination processes (which show an artifactual variation with heme concentration), we do not regard the trend in Table 1 toward longer lifetimes with increasing heme concentration as significant. We therefore adopt the 137-ns lifetime measured at 80 μM, the sample for which the best signal-to-noise was obtained, as the best estimate for the tertiary relaxation lifetime.

To compare the effect of low heme concentration on the lifetimes with those at the higher concentrations, we measured the lifetimes at a heme concentration of 8 μM. For this concentration of heme, the percentage in dimer is 35%. The four lifetimes obtained from SVD analysis and subsequent lifetime fitting to the time course of the basis spectra are shown with their corresponding amplitudes in Table 1. The results for 8 μM show no significant change for the lifetimes of the geminate recombination, tertiary relaxation, and the fast diffusional rebinding of O_2 from those found for 80 μM. However, the lifetime of the slow diffusional rebinding of O_2 has increased significantly for low heme concentration.

At low heme concentrations, we might expect to observe ligand recombination rates corresponding to photolyzed dimers, as well as to tetramers. We thus analyzed the 8 μM data in terms of additional exponential processes, for a total of five and six processes. The results for four, five, and six exponentials are shown in Table 2. The resolved lifetimes suggest simultaneous contributions of the dimeric and the tetrameric hemoglobin to the observed kinetics, as expected. They correspond to the four processes that are seen for the sample that is 80 μM in heme, as well as new lifetimes that are attributed to O_2 recombinations to dimeric hemoglobin. In particular, the six-exponential results suggest that the binding of O_2 to the α subunit of the dimer (63-μs lifetime) is two times slower than that of the tetramer. Similarly, the appearance of an 18-μs lifetime, intermediate between the β and α lifetimes of the tetramer, suggests a similar slowing of O_2 recombination to β chains in the dimer as well.

The rate constant for the binding of O_2 to the α subunit of hemoglobin dimer differs from that reported by Philo and Lary (1990). Although their reported values for the binding of O_2 to the β and the α subunits of the tetramer are consistent with the values we find at 80 μM heme concentration in Table 1, their conclusion that the β and α binding rates are not significantly different for the dimer is not

TABLE 2 Lifetimes (amplitudes)* for the relaxation of intermediate species formed through laser photolysis of human oxyhemoglobin at 532 nm

	τ_1	τ_2	τ_3	τ_4	τ_5	τ_6
Four-exponential processes	30 ns (0.54)	148 ns (0.04)	14 μs (0.06)	76 μs (0.34)		
Five-exponential processes	30 ns (0.48)	165 ns (0.04)	15 μs (0.08)	24 μs (0.12)	88 μs (0.27)	
Six-exponential processes	30 ns (0.25)	192 ns (0.01)	11 μs (0.1)	18 μs (0.31)	27 μs (0.15)	63 μs (0.15)

These lifetimes correspond to the heme concentration of 8 μM. The results are given for four-exponential, five-exponential, and six-exponential fit to the time course of the basis spectra resulting from the SVD analysis of the spectral matrix.
*Uncertainties associated with the above lifetimes (amplitudes) are approximately 10% of the tabulated numbers. For the low-amplitude processes the uncertainties might be higher than 10%.

supported by our results. They estimate an upper limit of about 15% difference between dimer and tetramer rate constants, in contrast to the factor of 2 difference in rate constant found here for the dimer.

Although we cannot specify the source of the discrepancy between our findings for the O_2 on rates of the dimer and those of Philo and Lary, we do point out that the new kinetic values appear to be more consistent with the extensive picture of subunit association and ligand binding thermodynamics assembled by Ackers and co-workers (Ackers and Johnson, 1990). In this picture, the ligand affinity of R_3 tetramer is expected to be about four times higher than that of isolated chains and $\alpha\beta$ dimer (quaternary enhancement). Although we cannot determine ligand affinities from our kinetic data (without ligand association rates), the higher ligand-binding rate constants of the tetramers are certainly suggestive of a quaternary enhancement in affinity for the α and β subunits (barring an increase in the ligand off rates that coincidentally offsets the increase in binding rate constants observed here).

SUMMARY

In summary, time-resolved absorption spectroscopy of the intermediate species produced through nanosecond laser photodissociation of oxyhemoglobin shows a small effective yield of photoproduct (as a consequence of geminate recombination and electronic relaxation processes that are too rapid for observation), followed by decay of the initial photoproduct through a slow geminate recombination, tertiary relaxation, and subsequent diffusional rebinding with molecular oxygen. The first-order and pseudo-first-order reactions of photoproducts were analyzed by application of singular value decomposition (SVD) and global kinetic fitting (exponential fitting of the time basis functions resulting from SVD analysis). At a heme concentration of 80 μM, we found four lifetimes, with mean values of 38 ns, 137 ns, 11 μs, and 31 μs. The first lifetime is due to the slow geminate recombination reaction and the second lifetime corresponds to the tertiary relaxation of the protein in the R-state quaternary structure. The last two lifetimes have been assigned by previous investigators to selective bimolecular binding of molecular oxygen to the β (Hb^R) and to the α (Hb^R) subunits of deoxyhemoglobin, respectively.

At lower heme concentrations, we make the new observation that α and β chains in Hb dimers rebind ligand with distinct second-order rate constants that are smaller than those for the chains in tetramers. This finding calls into question kinetic evidence from earlier studies for nearly identical ligand binding affinities for Hb dimers and tetramers, and thereby appears to resolve a previous discrepancy between the kinetic evidence and the evidence from many other, largely equilibrium, studies supporting the existence of a quaternary enhancement of ligand affinity in Hb tetramers (Ackers and Johnson, 1990).

We are grateful to Prof. Robert A. Alberty for helpful discussions and for a preprint of his work.

This work was supported by the National Institutes of Health (grants GM38549 and GM35158).

REFERENCES

Ackers, G. K., and M. L. Johnson. 1990. Analysis of hemoglobin oxygenation from combined equilibrium and kinetic data: is quaternary enhancement necessary? *Biophys. Chem.* 37:265–279.

Alben, J. O., G. H. Bare, and P. P. Moh. 1978. Fourier transform infrared spectroscopy of hemoglobin. *In* Biochemical and Clinical Aspects of Hemoglobin Abnormalities. W. S. Caughey, editor. Academic Press, New York. 607–617.

Alberty, R. A. 1991. Chemical equilibrium in complex organic systems with various choices of independent variables. *In* Chemical Reactions in Complex Mixtures. A. V. Sapre and F. J. Krambeck, editors. Van Nostrand Reinhold, New York. 227–298.

Alpert, B., S. El Mohsni, L. Lindqvist, and F. Tfibel. 1979. Transient effects in the nanosecond laser photolysis of carboxyhemoglobin: "cage" recombination and spectral evolution of the protein. *Chem. Phys. Lett.* 64:11–15.

Baldwin, J. M. 1980. The structure of human carbonmonoxy haemoglobin at 2.7 Å resolution. *J. Mol. Biol.* 136:103–128.

Bandyopadhay, D., D. Magde, T. G. Traylor, and V. S. Sharma. 1992. Quaternary structure and geminate recombination in hemoglobin: flow-flash studies on $\alpha_2^{co}\ \beta_2$ and $\alpha_2\ \beta_2^{co}$. *Biophys. J.* 63:673–681.

Chernoff, D. A., R. M. Hochstrasser, and A. W. Steele. 1980. Geminate recombination of O_2 and hemoglobin. *Proc. Natl. Acad. Sci. USA.* 77:5606–5610.

Demma, L. S., and J. M. Salhany. 1977. Direct generation of superoxide anions by flash photolysis of human oxyhemoglobin. *J. Biol. Chem.* 252:1226–1230.

Demma, L. S., and J. M. Salhany. 1979. Subunit inequivalence in superoxide anion formation during photoxidation of human oxyhemoglobin. *J. Biol. Chem.* 254:4532–4535.

Dennis, J. E., and D. J. Woods. 1987. Optimization on microcomputers: the Nelder-Mead simplex algorithm. *In* New Computing Environments:

Microcomputers in Large-Scale Computing. A. Wouk, editor. SIAM, Philadelphia. 116–122.

Duddell, D. A., R. J. Morris, N. J. Muttucumaru, and J. T. Richards. 1980. The dependence of the quantum yield of ligand photodissociation from haem proteins on ultrafast recombination. *Photochem. Photobiol.* 31: 479–484.

Duddell, D. A., R. J. Morris, and J. T. Richards. 1979. Ultra-fast recombination in nanosecond laser photolysis of carbonylhaemoglobin. *J. Chem. Soc. Chem. Commun.* 75–76.

Ferrone, F. A., A. J. Martino, and S. Basak. 1985. Conformational kinetics of triligated hemoglobin. *Biophys. J.* 48:269–282.

Friedman, J. M., and K. B. Lyons. 1980. Transient Raman study of CO-haemoprotein photolysis: origin of the quantum yield. *Nature.* 284: 570–572.

Friedman, J. M., T. W. Scott, G. J. Fisanick, S. R. Simon, E. W. Findsen, M. R. Ondrias, and V. W. Macdonald. 1985. Localized control of ligand binding in hemoglobin: effect of tertiary structure on picosecond geminate recombination. *Science.* 229:187–190.

Geraci, G., L. J. Parkhurst, and Q. H. Gibson. 1969. Preparation and properties of α and β chains from human hemoglobin. *J. Biol. Chem.* 17:4664–4667.

Gibson, Q. H. 1959. The photochemical formation of quickly reacting form of hemoglobin. *Biochem. J.* 71:293–303.

Gibson, Q. H. 1973. The contribution of the α and β chains to the kinetics of oxygen binding to and dissociation from hemoglobin. *Proc. Natl. Acad. Sci. USA.* 70:1–4.

Gibson, Q. H., M. Ikeda-Saito, and T. Yonetani. 1985. Geminate reactions of oxygen and nitric oxide with the α and β subunits of Fe-Co hybrid hemoglobins. *J. Biol. Chem.* 260:14126–14131.

Goldbeck, R. A., S. J. Paquette, S. C. Björling, and D. S. Kliger. 1996. Allosteric intermediates in hemoglobin. 2. Kinetic modeling of HbCO photolysis. *Biochemistry.* 35:8628–8639.

Golub, G. H., and C. Reinsch. 1970. Singular value decomposition and least squares solutions. *Num. Math.* 14:403–415.

Hager, W. W. 1988. Applied Numerical Linear Algebra. Prentice Hall, Englewood Cliffs. 294–302.

Hayashi, A., T. Suzuki, and M. Shin. 1973. An enzymatic reduction system for metmyoglobin and methemoglobin, and its application to functional studies of oxygen carriers. *Biochim. Biophys. Acta.* 310:309–315.

Hofrichter, J., E. R. Henry, J. H. Sommer, R. Deutsch, M. Ikeda-Saito, T. Yonetani, and W. A. Eaton. 1985. Nanosecond optical spectra of iron-cobalt hybrid hemoglobins: geminate recombination, conformational changes, and intersubunit communication. *Biochemistry.* 24:2667–2679.

Hofrichter, J., J. H. Sommer, E. R. Henry, and W. A. Eaton. 1983. Nanosecond absorption spectroscopy of hemoglobin: elementary processes in kinetics cooperativity. *Proc. Natl. Acad. Sci. USA.* 80: 2235–2239.

Hopfield, J. J. 1973. Relation between structure, co-operativity and spectra in a model of hemoglobin action. *J. Mol. Biol.* 77:207–222.

Jameson, G. B., and J. A. Ibers. 1994. Biological and synthetic dioxygen carriers. *In* Bioinorganic Chemistry. I. Bertini, H. B. Gray, S. J. Lippard, and J. S. Valentine, editors. University Science Books, Mill Valley, CA. 167–252.

Jayaraman, V., K. R. Rodgers, I. Mukerji, and T. G. Spiro. 1995. Hemoglobin allostery: resonance Raman spectroscopy of kinetic intermediates. *Science.* 269:1843–1848.

Johnson, M. L., H. R. Halvorson, and G. K. Ackers. 1976. Oxygenation-linked subunit interactions in human hemoglobin: analysis of linkage functions for constituent energy terms. *Biochemistry.* 15:5363–5371.

Jones, C. M., A. Ansari, E. R. Henry, G. W. Christoph, J. Hofrichter, and W. A. Eaton. 1992. Speed of intersubunit communication in proteins. *Biochemistry.* 31:6692–6702.

Koshland, D. E., G. Nemethy, and D. Filmer. 1966. Comparison of experimental binding data and theoretical models in proteins containing subunits. *Biochemistry.* 5:365–385.

Krambeck, F. J. 1991. Continuous mixtures in fluid catalytic cracking and extensions. *In* Chemical Reactions in Complex Mixtures. A. V. Sapre and F. J. Krambeck, editors. Van Nostrand Reinhold, New York. 42–59.

Lambright, D. G., S. Balasubramanian, and S. G. Boxer. 1991. Protein relaxation dynamics in human myoglobin. *Chem. Phys.* 158:249–260.

Lewis, J. W., and D. S. Kliger. 1991. Rotational diffusion effects on absorbance measurements: limitations to the magic-angle approach. *Photochem. Photobiol.* 54:963–968.

Lim, M., T. A. Jackson, and P. A. Anfinrud. 1995. Binding of CO to myoglobin from a heme pocket docking site to form nearly linear Fe-C-O. *Science.* 269:962–966.

Lindqvist, L., M. P. Fontaine, E. Bréheret, B. Alpert, and J. C. Andre. 1983. Photodissociation of oxyhemoglobin by nanosecond laser excitation: study of the geminate recombination kinetics. *In* Photochemistry and Photobiology, Vol. 2. A. H. Zewail, editor. Harwood, New York. 811–816.

Mills, F. C., M. L. Johnson, and G. K. Ackers. 1976. Oxygenation-linked subunit interactions in human hemoglobin: experimental studies on the concentration dependence of oxygenation curves. *Biochemistry.* 15: 5350–5362.

Monod, J., J. Wyman, and J. P. Changeux. 1965. On the nature of allosteric transitions: a plausible model. *J. Mol. Biol.* 12:88–118.

Morris, R. J., Q. H. Gibson, M. Ikeda-Saito, and T. Yonetani. 1984. Geminate combination of oxygen with iron-cobalt hybrid hemoglobins. *J. Biol. Chem.* 259:6701–6703.

Noble, R. W., Q. H. Gibson, M. Brunori, E. Antonini, and J. Wyman. 1969. The rates of combination of the isolated chains of human hemoglobin with oxygen. *J. Biol. Chem.* 244:3905–3908.

Pauling, L. 1935. The oxygen equilibrium of hemoglobin and its structural interpretation. *Proc. Natl. Acad. Sci. USA.* 21:186–191.

Pauling, L. 1964. Nature of the iron-oxygen bond in oxyhaemoglobin. *Nature.* 203:182–183.

Philo, J. S., and J. W. Lary. 1990. Kinetic investigations of the quaternary enhancement effect and α/β differences in binding the last oxygen to hemoglobin tetramers and dimers. *J. Biol. Chem.* 265:139–143.

Sawicki, C. A., and Q. H. Gibson. 1977. Quaternary conformational changes in human oxyhemoglobin studied by laser photolysis. *J. Biol. Chem.* 252:5783–5788.

Sawicki, C. A., and Q. H. Gibson. 1981. Tetramer-dimer dissociation of carboxyhemoglobin in the absence of dithionite. *Biophys. J.* 35: 265–270.

Scott, T. W., and J. M. Friedman. 1984. Tertiary-structure relaxation in hemoglobin: a transient Raman study. *J. Am. Chem. Soc.* 106: 5677–5687.

Shaanan, B. 1982. The iron-oxygen bond in human oxyhaemoglobin. *Nature.* 296:683–684.

Shibayama N., T. Yonetani, R. M. Regan, and Q. H. Gibson. 1995. Mechanism of ligand binding to Ni(II)-Fe(II) hybrid hemoglobins. *Biochemistry.* 34:14658–14667.

Spiro, T. G., G. Smulevich, and C. Su. 1990. Probing protein structure and dynamics with resonance Raman spectroscopy: cytochrome *c* peroxidase and hemoglobin. *Biochemistry.* 29:4497–4508.

Terner, J., J. D. Stong, T. G. Spiro, M. Naguma, M. Nicol, and M. A. El-Sayed. 1981. Picosecond resonance Raman spectroscopic evidence for excited-state spin conversion in carbonmonoxy-hemoglobin photolysis. *Proc. Natl. Acad. Sci. USA.* 78:1313–1317.

Woodruff, W. H., and S. Farquharson. 1978. Time-resolved resonance Raman spectroscopy of hemoglobin derivatives: heme structure changes in 7 nanoseconds. *Science.* 201:831–833.

Yu, N.-T. 1986. Resonance Raman studies of ligand binding. *Methods Enzymol.* 130:350–409.